AD-A125 511 GRAPHITE ABLATION IN SEVERAL GAS ENVIRONMENTS(U) JOHNS HOPKINS UNIV LAUREL MD APPLIED PHYSICS LAB R W NEWMAN ET AL. JAN 83 JHU/APL/TG-1336 1/1

UNCLASSIFIED N00024-83-C-5301 F/G 11/4 NL

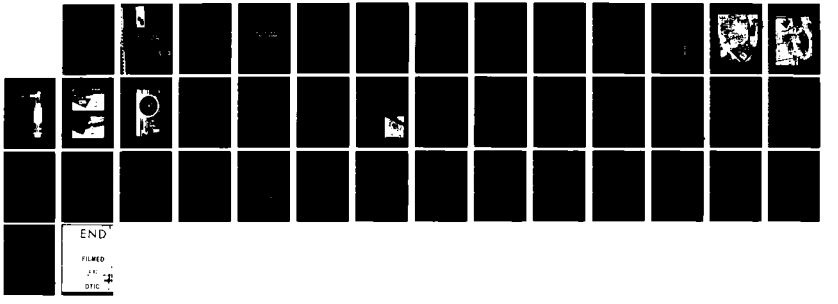

END

FILMED

DTIC

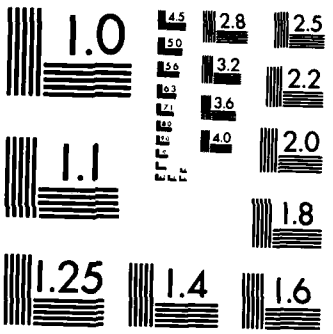

JHU/APL
TG 1336
JANUARY 1983
Copy No. 1

12

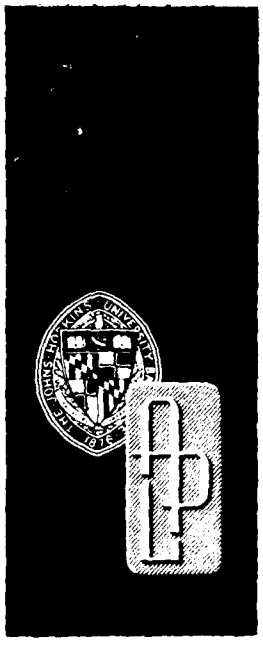

Technical Memorandum

GRAPHITE ABLATION IN SEVERAL GAS ENVIRONMENTS

R. W. NEWMAN
C. H. HOSHALL

THE JOHNS HOPKINS UNIVERSITY ■ APPLIED PHYSICS LABORATORY

PLEASE FOLD BACK IF NOT NEEDED FOR BIBLIOGRAPHIC PURPOSES

REPORT DOCUMENTATION PAGE

1. REPORT NUMBER	2. GOVT ACCESSION NO.	3. RECIPIENT'S CATALOG NUMBER
JHU/APL TG 1336		

4. TITLE (*and Subtitle*)
GRAPHITE ABLATION IN SEVERAL GAS ENVIRONMENTS

5. TYPE OF REPORT & PERIOD COVERED
Technical Memorandum

6. PERFORMING ORG. REPORT NUMBER
JHU/APL TG 1336

7. AUTHOR (*s*)
R. W. Newman and C. H. Hoshall

8. CONTRACT OR GRANT NUMBER (*s*)
N00024-83-C-5301

9. PERFORMING ORGANIZATION NAME & ADDRESS
The Johns Hopkins University Applied Physics Laboratory
Johns Hopkins Road
Laurel, MD 20707

10. PROGRAM ELEMENT, PROJECT, TASK AREA & WORK UNIT NUMBERS
Task X8G1

11. CONTROLLING OFFICE NAME & ADDRESS
Naval Plant Representative Office
Johns Hopkins Road
Laurel, MD 20707

12. REPORT DATE
January 1983

13. NUMBER OF PAGES
42

14. MONITORING AGENCY NAME & ADDRESS
Naval Plant Representative Office
Johns Hopkins Road
Laurel, MD 20707

15. SECURITY CLASS. (*of this report*)
Unclassified

15a. DECLASSIFICATION/DOWNGRADING SCHEDULE

16. DISTRIBUTION STATEMENT (*of this Report*)
Approved for public release; distribution unlimited.

17. DISTRIBUTION STATEMENT (*of the abstract entered in Block 20, if different from Report*)

18. SUPPLEMENTARY NOTES

19. KEY WORDS (*Continue on reverse side if necessary and identify by block number*)
ablation
carbon-carbon composite
diffusion limit
combustor
graphite

20. ABSTRACT (*Continue on reverse side if necessary and identify by block number*)

The design of a passively cooled combustor for a hypersonic tactical missile poses many severe structural problems whose solutions are beyond the current state of the art. To design such a combustor, the designer must predict accurately the erosion rate of candidate materials so that a realistic balance can be achieved among weight, performance, and cost. To make these predictions, basic experimental data must be taken to determine ablation rates as a function of surface temperature, pressure, gas flow rate, and gas composition. An experimental procedure has been developed to obtain this information for graphite materials exposed to various gases, such as CO, CO_2, argon, and H_2O, and simulated Shelldyne H-air combustion products. The data agree well with data obtained from the literature and indicate that at temperatures above 3500°F (a) the ablation rate is diffusion limited, (b) CO_2 in the stream reacts with carbon at the surface to form CO, and (c) water vapor reacts with the surface (this was not anticipated prior to the tests). At 2000°F, ablation is controlled by reaction rate, and both CO_2 and water vapor in the stream react with the surface.

DD FORM 1 JAN 73 **1473**

JHU/APL
TG 1336
JANUARY 1983

Technical Memorandum

GRAPHITE ABLATION IN SEVERAL GAS ENVIRONMENTS

R. W. NEWMAN
C. H. HOSHALL

THE JOHNS HOPKINS UNIVERSITY ■ APPLIED PHYSICS LABORATORY
Johns Hopkins Road, Laurel, Maryland 20707
Operating under Contract N00024-83-C-5301 with the Department of the Navy

ABSTRACT

The design of a passively cooled combustor for a hypersonic tactical missile poses many severe structural problems whose solutions are beyond the current state of the art. The designer of such a combustor must predict accurately the erosion rate of candidate materials so that a realistic balance can be achieved among weight, performance, and cost. To make these predictions, basic experimental data must be taken to determine ablation rates as functions of surface temperature, pressure, gas flow rate, and gas composition.

An experimental procedure has been developed to obtain ablation data for graphite materials, and tests have been performed on ATJ graphite samples. ATJ graphite was chosen because it has well-documented ablation properties that can be used to evaluate the accuracy of our test procedure. For these tests, ATJ graphite pellets, 3.3 mm in diameter, were electrically heated to temperatures between 2000 and 4500°F. Reacting gases flowed perpendicularly to the surface at velocities between 1 and 20 m/s. whe gases simulated Shelldyne-air combustion products at fuel-air equivalence ratios from 0.0 to 1. In addition, the effects on ablation of oxygen, carbon monoxide, carbon dioxide, argon, and water vapor were evaluated. The sample's surface temperature was measured with an optical pyrometer, and average ablation rates were determined from changes in specimen thickness and weight during each test.

The results of 40 tests are reported. The data agree well with results obtained from the literature and indicate that at temperatures above 3500°F (a) the ablation rate is diffusion limited, (b) carbon dioxide in the stream reacts with carbon at the surface to form carbon monoxide, and (c) water vapor apparently reacts with the surface. At 2000°F, ablation is reaction-rate controlled, and both carbon dioxide and water vapor in the stream react with the surface.

Thus, a procedure for such testing has been developed and proven. Recommendations for testing other materials such as carbon-carbon composites are included. Also discussed are procedures for measuring species concentrations near the surface using Raman scattering techniques in conjunction with this test arrangement.

THE JOHNS HOPKINS UNIVERSITY
APPLIED PHYSICS LABORATORY
LAUREL, MARYLAND

PREFACE

The purpose of this report is to describe the experimental arrangement and test procedure used to measure ablation rates on ATJ graphite test specimens. Test results are reported and, in some cases, compared to analytical results.

This work has been supported during 1981 and 1982 by in-house research and development funding.

CONTENTS

ILLUSTRATIONS

TABLES

1. INTRODUCTION

Carbon-based materials are used in thermal protection systems for reentry vehicles and missiles. The design of hypersonic tactical missile combustors poses many severe structural problems whose solutions challenge the current state of the art. To design such a combustor, the designer must predict accurately the erosion rate of candidate materials so that a realistic balance can be achieved among weight, performance, and cost. To make these predictions, basic experimental data must be taken to determine ablation rates as functions of surface temperature, pressure, gas flow rate, and gas composition.

The primary objective of this test program was to determine ablation rates for ATJ graphite samples exposed to various conditions and to use those rates to evaluate an analytical model of ATJ ablation in a combustor environment. Preliminary tests indicated that a test apparatus could be built to measure the ablation rates,[1] and a test plan giving the required test conditions[2] was developed. This report describes the test apparatus, the test results, and plans for ongoing work.

[1] C. H. Hoshall, *Graphite Ablation Tests,* JHU/APL CFP-80-003 (15 Jan 1980).

[2] R. W. Newman, *Test Plan to Measure High Temperature Graphite Ablation Rate,* JHU/APL EM-4999 (26 Jun 1981).

2. SUMMARY

The apparatus developed in late 1979 in the APL Combustion Research Laboratory[1] was modified for the current series of tests. Figure 1 is a block diagram of the apparatus as it was at the end of the tests; Figs. 2 through 7 are photographs of various parts of the test setup and ancillary apparatus.

Specimen temperatures up to 4500°F are achievable with the electrically heated graphite electrode. Specimens of ATJ graphite, approximately 0.13 in. (3.3 mm) in diameter and 0.07 in. (1.78 mm) thick (Fig. 5), are placed in a graphite guard ring; the assembly is put into a shallow cylindrical recess at the tip of the heater and heated by conductive and radiative energy transfer from the heater. Specimens can be heated this way to 4000°F; with less reliability, they can be heated to 4500°F. Reagent gases exit from the nozzle, which is normal to the flat surface of the specimen (Figs. 1 and 3). The numbers in the triangles in Fig. 3 correspond to the numbers identified in Fig. 1.

Tests were run at temperatures ranging from 2000 to 4500°F with incident gas flow rates from 1.2 to 22 m/s. Air, oxygen (O_2), carbon dioxide (CO_2), and carbon monoxide (CO) were used as reagents. Some tests were run with "dry" reagents whose water contents were typical of compressed gases. The water contents of the compressed gases were not measured; however, on the basis of information from the supplier, typical water contents at 2000 psia are 17 ppm for air, 8 ppm for O_2, 128 ppm for CO_2, and 2 ppm for CO. For some tests, water vapor was added in known amounts. Also, mixtures of nitrogen (N_2), O_2, CO_2, CO, and water vapor were used to simulate the products of combustion of Shelldyne-H fuel burned at equivalence ratios (*ER*'s) ranging from approximately 0.3 to 1.0.

A summary of test conditions and results for the 40 tests reported herein is presented in Tables 1 and 2. The results agree well with data in the literature for air and CO_2. CO_2 and water both react with the ATJ graphite surface, even at temperatures as low as 2000°F.

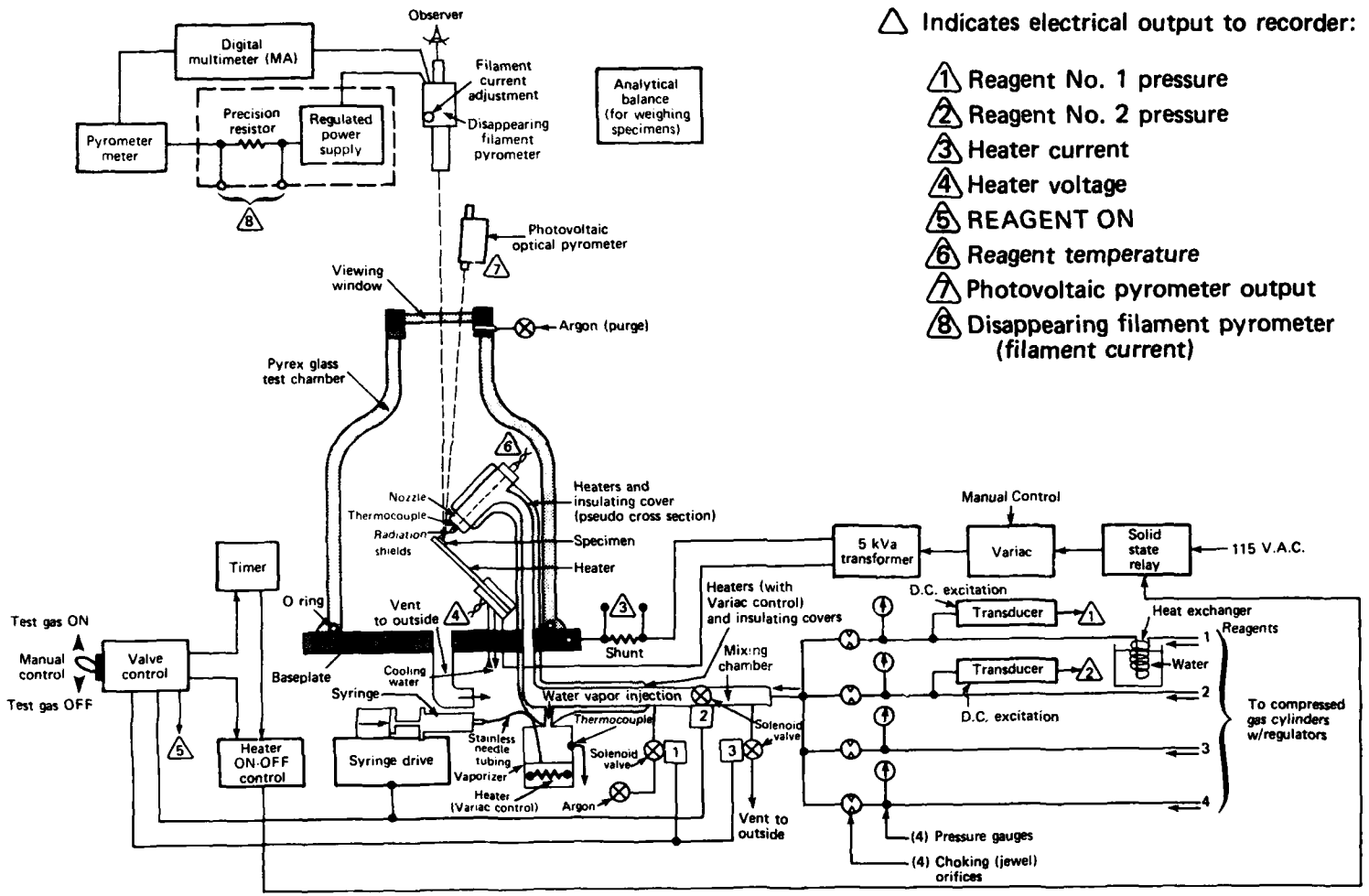

Figure 1 — Block diagram of test apparatus for graphite reaction measurements.

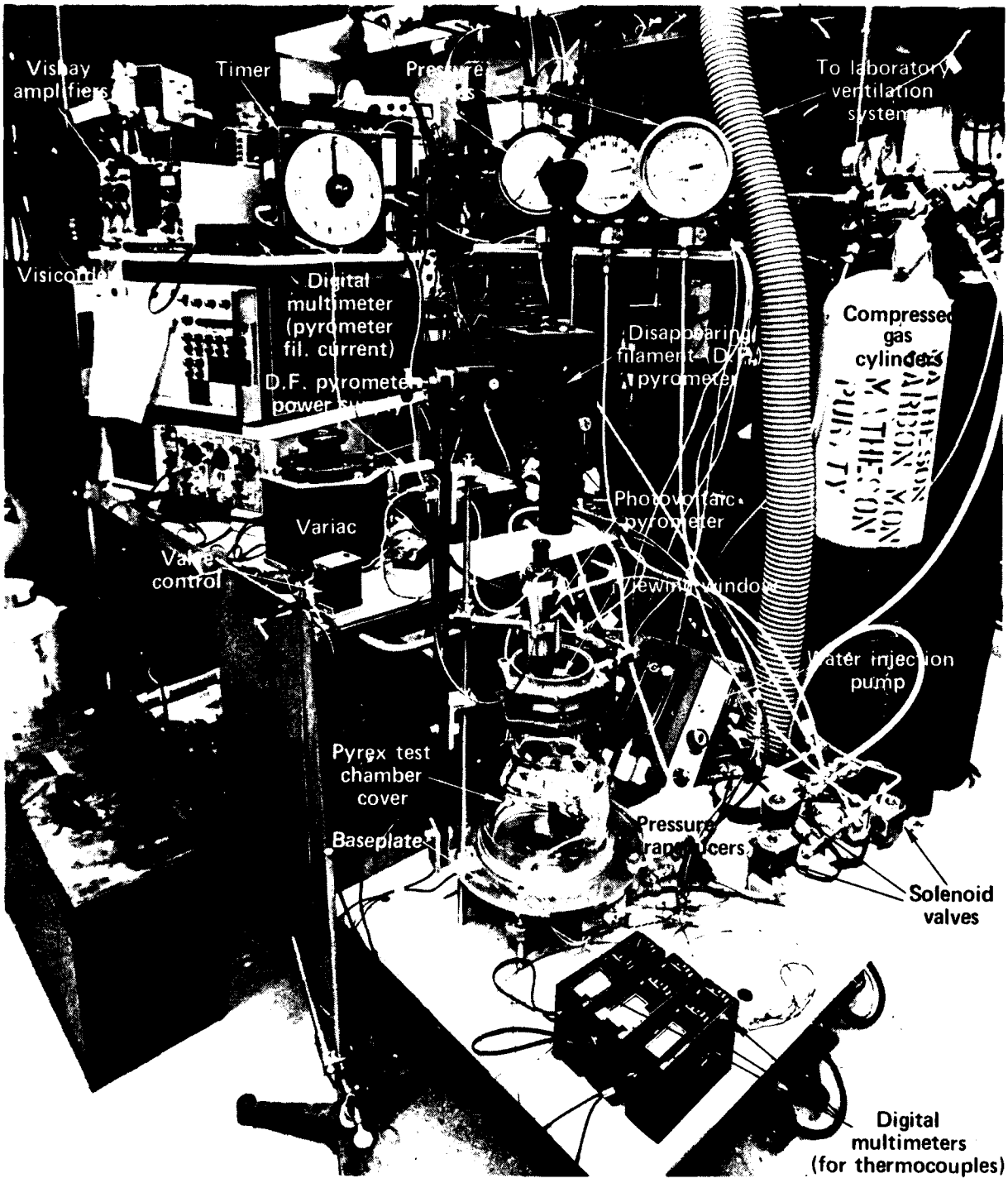

Figure 2 — Graphite ablation apparatus (Pyrex cover in place).

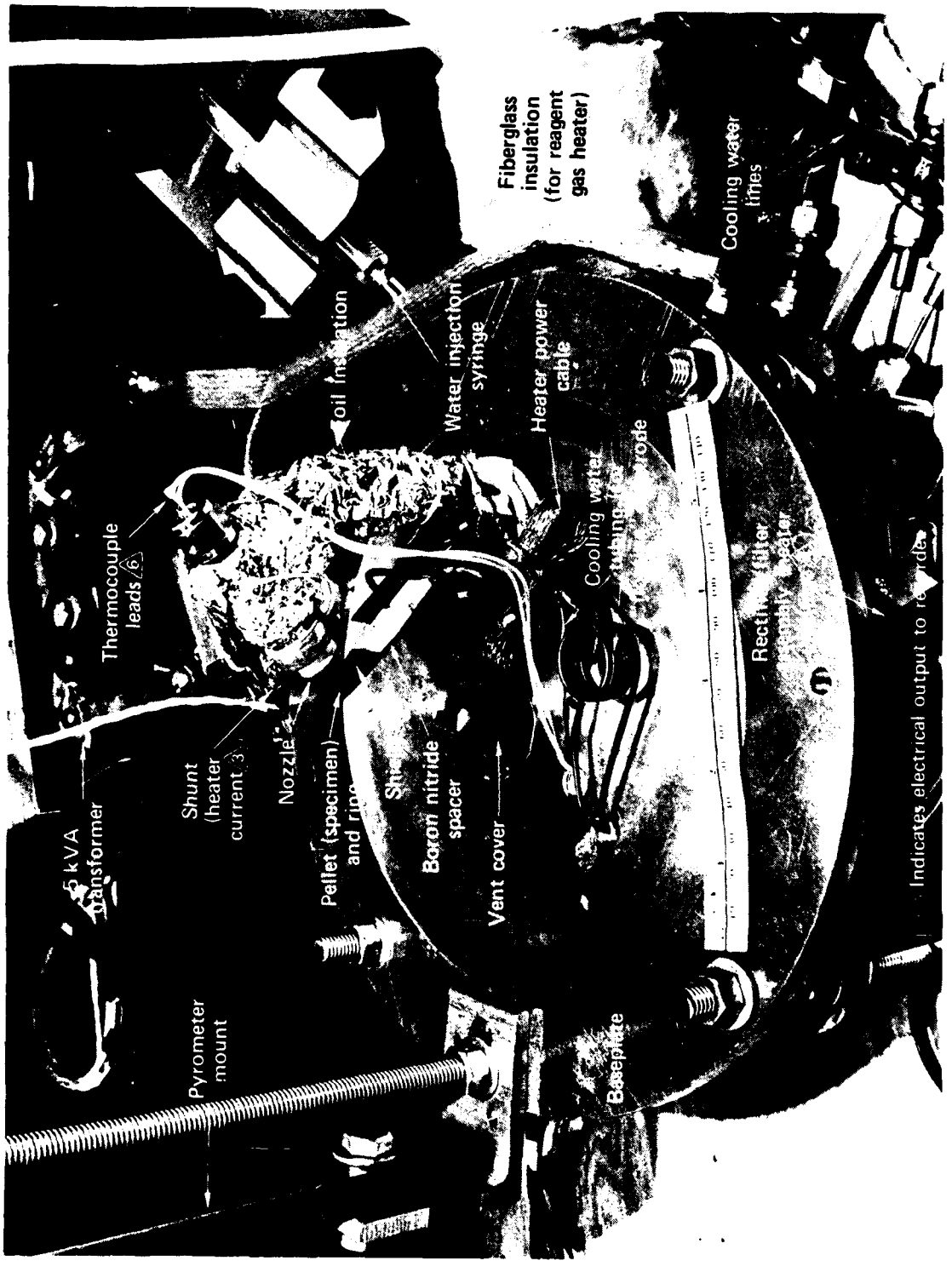

Figure 3 — Closeup of apparatus (Pyrex cover removed).

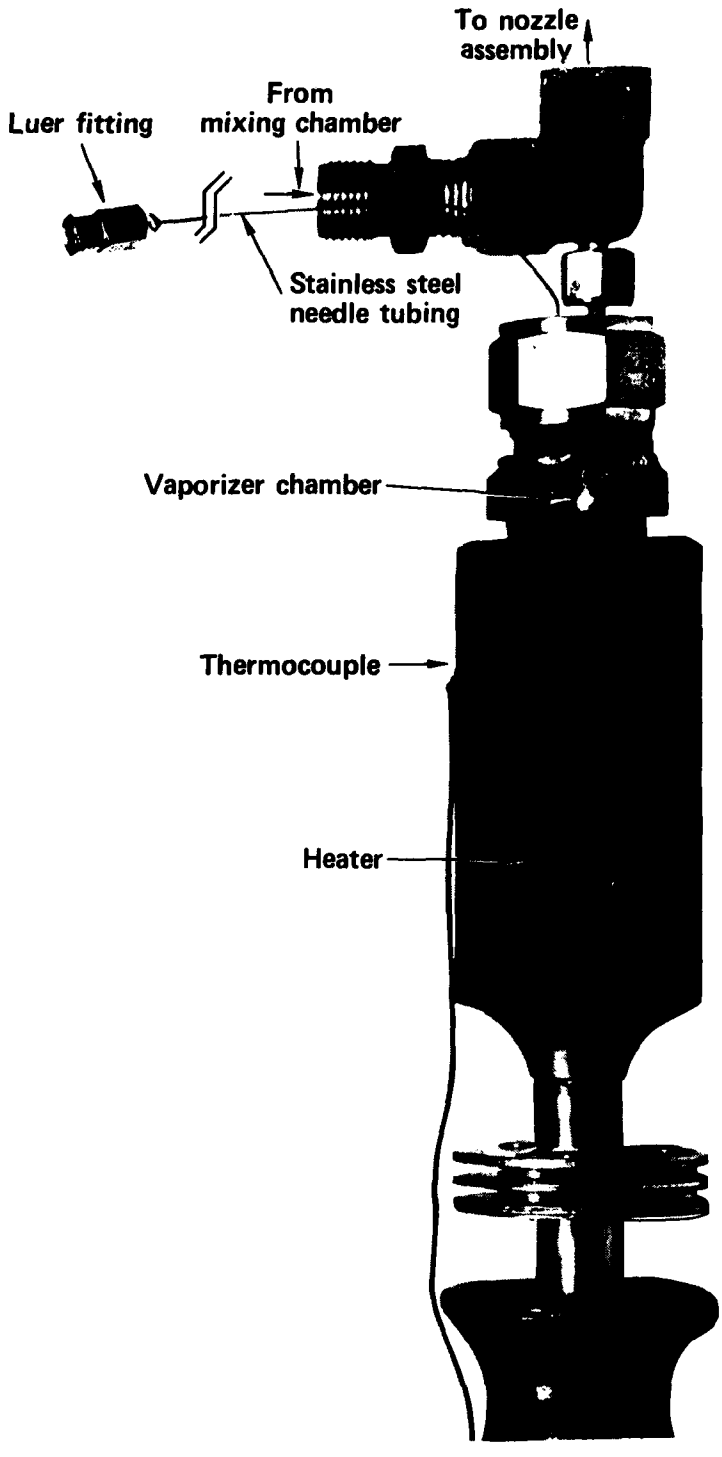

Figure 4 — Vaporizer assembly.

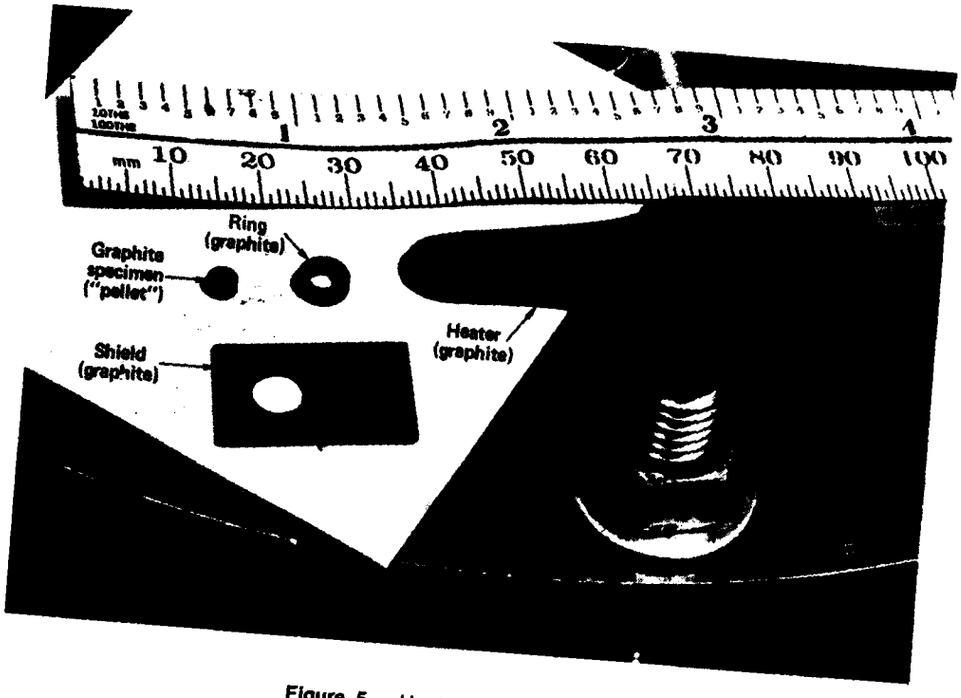

Figure 5 — Heater, specimen, and shield.

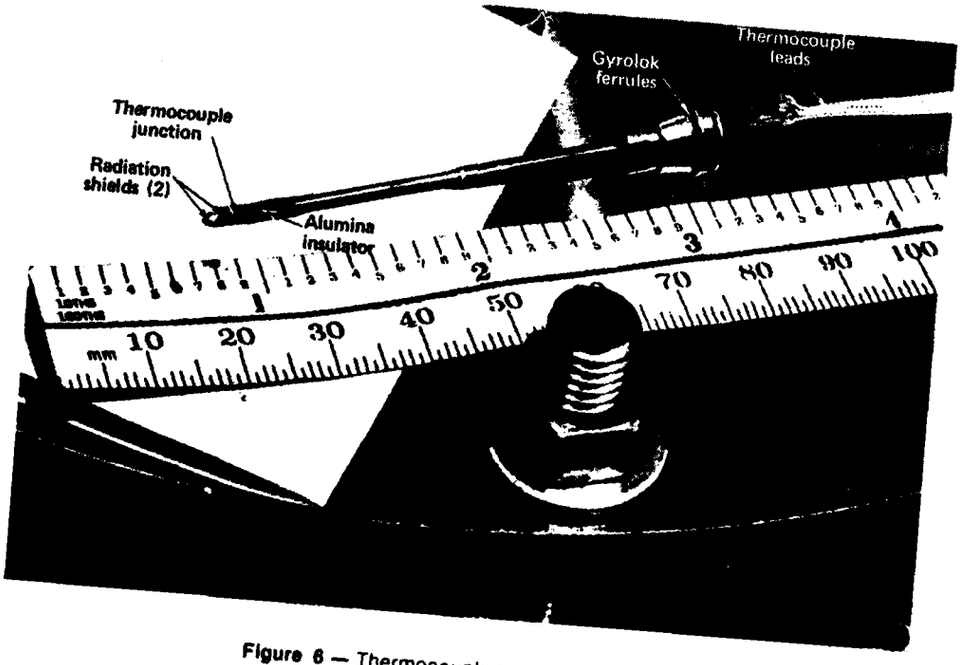

Figure 6 — Thermocouple assembly (for nozzle).

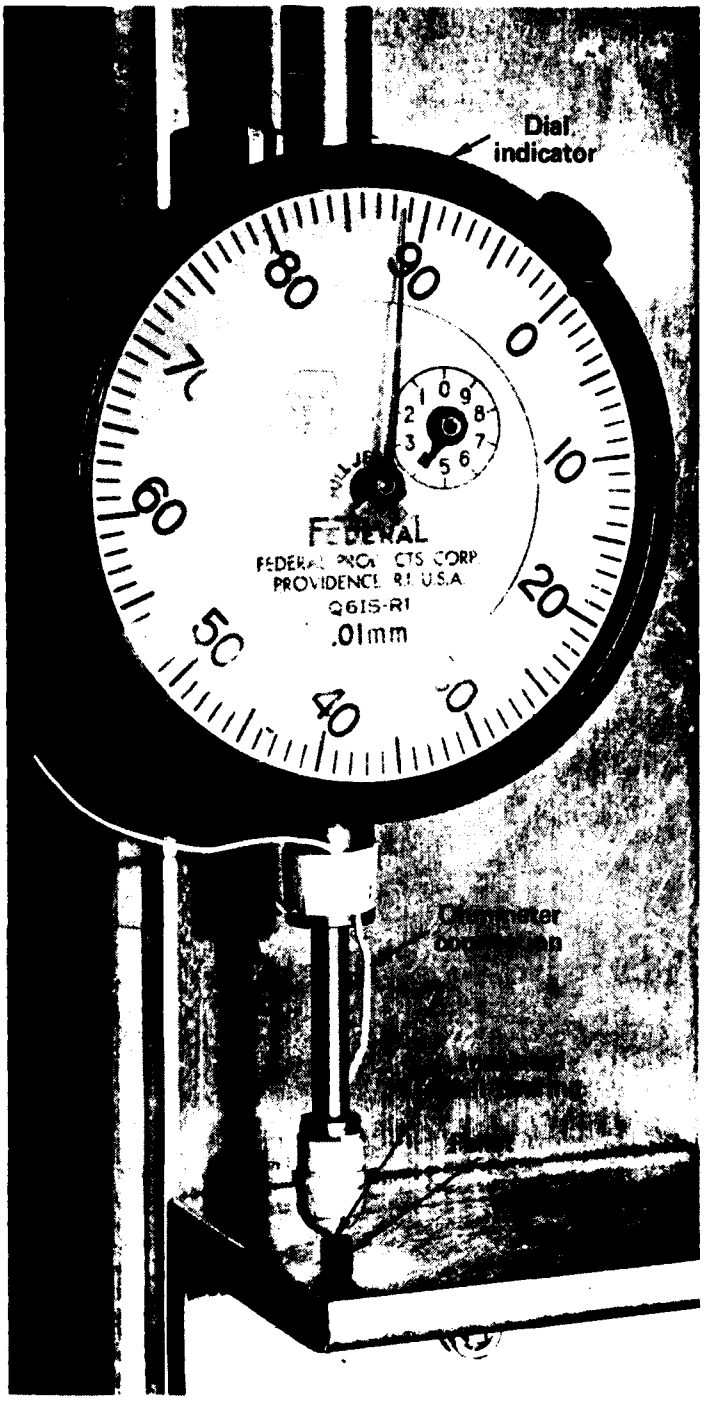

Figure 7 — Device for measuring specimen thickness.

Table 1 – ATJ graphite ablation test summary (1981 tests).

Test No.	ATJ Temp. (°F)	Gas	Water[a] (vol. %)	Gas Velocity (m/s)		Test Duration (s)	Mass Transfer Parameter β'	Recession Rate (mil/s)	
				Nominal[b]	Computed			$\dot{y}_m$	$\dot{y}_t$
1	4000	Air		10	12.5	27	0.134	0.63	0.53
2	4000	Air		10	12.5	30	0.140	0.66	0.61
3	3500	Air		1	1.98	30	0.174	0.27	0.21
4	2000	Air		0.99	1.18	120	0.134	0.16	0.14
5	4130	Air		0.99	2.33	45	0.155	0.26	0.20
6	4170	Air		1		75			0.33
7	4000	Air		1		75			0.34
8	4000	Air		1	2.37	75	0.154	0.26	0.23
9	4000	Air	6.5%	1	2.37	81	0.178	0.29	0.28
10	4000	Air	6.5%	1	2.37	105	0.179	0.29	0.22
11	3500	Air	6.5%	1	2.01	120	0.210	0.33	0.26
12	2000	Air	6.5%	1	1.16	180	0.126	0.16	0.14
13	2500	Air	6.5%	1	1.28	210	0.131	0.18	0.16
14	3000	Air	6.5%	1	1.63	180	0.176	0.26	0.24
15	4550	Air	6.5%	1	2.33	64	0.196	0.33	0.26
16	3500	Air		17	19.9	60	0.174	0.96	0.89
17	3500	Air		16.6	19.5	35	0.181	1.04	0.98
18	3500	Air	6.5%[c]	16.6	19.5	25	0.191	1.09	0.98
19	3500	Air	[d]	17	19.5	25	0.197	1.12	0.99
20	3500	Air	4.5%	16.6	19.9	30	0.179	1.02	0.90

Table 1 – (cont'd)

Test No.	ATJ Temp. (°F)	Gas	Water[a] (vol. %)	Gas Velocity (m/s)		Test Duration (s)	Mass Transfer Parameter β'	Recession Rate (mil/s)	
				Nominal[b]	Computed			$\dot{y}_m$	$\dot{y}_t$
21	2000	Air	4.5%	16.6	17.4	30	0.093	0.49	0.38
22	3500	$ER = 0.3$[e]		20	22.5	40	0.165	1.04	0.90
23	3500	$ER = 0.3$[e]		20	22.5	40	0.172	1.08	1.02
24	2000	$ER = 0.3$[e]		1	1.18	120	0.103	0.14	0.10
25	3500	$ER = 0.3$[e]		1	2.01	77	0.150	0.24	0.17
26	3500	$ER = 0.3$[e]		1	2.01	180	0.153	0.25	0.21
27	2000	$ER = 0.6$[e]		1	1.18	300	0.0802	0.11	0.097
28	3500	$ER = 0.6$[e]		1	2.48	240	0.103	0.19	0.17
29	3500	$ER = 0.6$[e]		1	2.48	200	0.117	0.22	0.19
30	2000	$ER = 1.0$[e]		1	1.16	450	0.021	0.028	0.017
31	3500	$ER = 1.0$[e]		1	2.48	337	0.079	0.13	0.11
32	3500	CO_2	6.5%	1	2.48	116	0.176	0.35	0.30
33	2000	CO_2	6.5%	1	1.16	240	0.020	0.032	0.002
34	3500	CO_2	Dry	1	2.48	120	0.117	0.24	0.19
35	3500	CO	6.5%	1	2.48	420	0.032	0.052	0.042
36	3500	O_2	6.5%	1	2.48	24	0.888	1.19	1.10
37	3500	Ar	6.5%	1	2.48	253	0.26	0.059	0.043
38	4500	CO_2	6.5%	1	2.48	33	0.156	0.33	0.18
39	3500	$ER = 1.0$[c]		1	2.48	300	0.089	0.15	0.12
40	4000	$ER = 1.0$[c]		1	2.48	240	0.081	0.14	0.11

[a] Water content indicated is percent by volume of total (gas plus water). "Air" and "CO_2 dry" contain < 400 ppm water (< 0.04% by volume).

[b] Based on room-temperature exit gas from nozzle.

[c] There may have been less water vapor in the last part of the test.

[d] Water content is uncertain.

[e] Simulated as products of combustion (N_2, O_2, CO_2, CO, H_2O) for Shelldyne-H fuel; see Table 3.

Table 2 – Summary of conditions under which tests 1 through 40 were run.

Gas Conditions	*Nominal Gas Velocity* for Sample Temperature*									
	2000°F		*2500°F*	*3000°F*	*3500°F*			*4000°F*		*4500°F*
	1 m/s	*16.6 m/s*	*1 m/s*	*1 m/s*	*1 m/s*	*16.6 m/s*	*20 m/s*	*1 m/s*	*10 m/s*	*1 m/s*
Air										
<400 ppm H_2O	4				3	16, 17		5, 6, 7, 8	1, 2	
4.5% H_2O		21				20				
6.5% H_2O	12		13	14	11	18†, 19††		9, 10		15
Simulated Shelldyne-air										
ER = 0.3	24				25, 26		22, 23			
ER = 0.6	27				28, 29					
ER = 1.0	30				31, 39			40		
O_2										
6.5% H_2O					36					
CO_2										
<400 ppm H_2O					34					
6.5% H_2O	33				32					38
CO										
6.5% H_2O					35					
Argon										
6.5% H_2O					37					

*Based on room-temperature exit gas from nozzle.
†There may have been less water vapor in last part of test.
††Water content uncertain.

3. TEST APPARATUS DESIGN CONSIDERATIONS

One objective of this effort was to measure graphite ablation rates under conditions for which data were not available in the literature or in which there is special interest relating to the study of high-temperature thermochemical reactions of graphite. Another objective was to develop an apparatus and techniques that – in addition to their purpose in this series of tests – could aid planned future investigations using Raman scattering to measure species concentrations in the reaction zones near the surface of heated graphite.

The graphite specimen, ring, and shield assembly (Fig. 5) presents a continuous surface to the gas so that the pellet (specimen) will be uniformly ablated without undesired edge effects. The assembly rests on an electric resistance heater consisting of a 0.065 in. (1.65 mm) thick graphite sheet, 0.75 in. (1.91 cm) wide and 2.5 in. (6.35 cm) long, with a saw cut along most of its length to form a U-shaped resistor. The top of the heater (Fig. 5) is counterbored to a depth of approximately 0.030 in. (0.76 mm) to provide a positive support for the specimen and to help keep it from being blown away by the reagent gases. Water-cooled "jaws" provide the electric connections and support the heater electrode. One set of jaws is mounted on coiled stainless steel tubing (Fig. 3) to allow one leg of the heater to move freely. This provides minimal resistance to movement resulting from unequal expansion of the two legs of the heater; the legs can expand without breaking as they would do if they were supported rigidly.

A nozzle, 0.5 in. (12.7 mm) ID, is used to reduce the possibility of undesirable effects of contamination of the reagents as a result of the entrainment of gases present in the enclosure and diffusion of the ambient environments into the gas stream. It also ensures stagnation flow conditions across the entire surface of the 0.22 in. (5.6 mm) diameter specimen-guard ring assembly. The exit plane of the nozzle is 0.43 in. (11 mm) from the surface of the specimen.

To ensure that the gases are not substantially below room temperature as a result of adiabatic expansion (as the gases are released from the compressed gas cylinders), the gas supply line is fitted with a simple heat exchanger made of coiled copper tubing immersed in a container of water at room temperature (Fig. 1).

A simple apparatus has been made for injecting water vapor into the gas stream. A well-controlled flow of water vapor can be introduced into the test gas by means of a soldering iron heating element (Fig. 4) to supply heat and a commercial syringe pump (Fig. 2) to inject water at the required rate through small-gauge stainless steel tubing into the vaporizer. However, the output capacity is limited; consequently, tests with high water content (5 to 10%) were limited to 1 m/s velocity. Also, because of the limited water vaporization capacity, an accurate simulation of the Shelldyne-air combustion products for the $ER = 1$ condition (which requires 9.2% water) could only be achieved for a flow velocity of 1 m/s. To prevent condensation from occurring in the inlet piping and nozzle assembly, these parts were wrapped with heating tape.

A data acquisition system recorded all data measured during the tests. Eight channels of a Honeywell Model 1858 CRT Visicorder were used to record the analog voltages indicated in Fig. 1. A detailed description of each channel is provided in Appendix A.

Accurate measurement of the ablation is difficult because a lower-density layer is formed near the surface when ablation first starts. This lower-density layer is evident in an electron microscope photograph of a specimen's cross section (Fig. 8). The thickness of the layer was determined to be about 0.008 in.

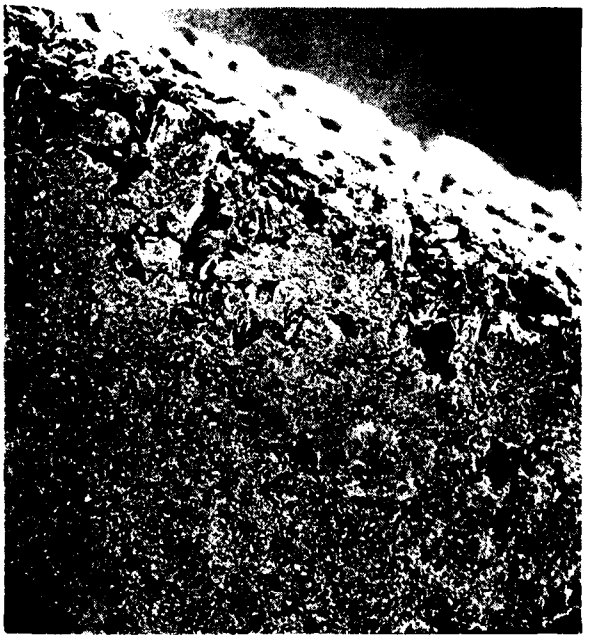

Figure 8 — Scanning electron microscope image of ATJ pellet after test.

(0.20 mm), and it was easily compressed when a micrometer measurement was attempted. To overcome this problem and to obtain an accurate measurment of the pellet thickness, the special device shown in Fig. 7 was made and was found to work satisfactorily. The wire that can be seen emerging along the stem of the dial indicator is attached to a small ball bearing epoxied to the indicator stem. By means of an ohmmeter, very light contact with the specimen surface can be detected easily. Specimen temperatures were measured using the disappearing filament pyrometer described in Appendix B.

4. TEST PROCEDURE

The general test procedure is as follows:

1. The pellet sample is weighed on an analytical balance and is measured with a micrometer. Then it is installed in the guard ring and electric heater.
2. Power to the heater is supplied by a 5 kVA transformer and is manually controlled by a Variac.
3. The desired amount of each reagent gas is metered through a choking orifice. The gases are mixed in a chamber, and flow of the gases is begun and stopped by solenoid valves. Unreacted gases and products of combustion leave the bell jar through a 1-in.-diameter hole in the baseplate directly beneath the tip of the heater and pass into the laboratory's vent system. The solenoid valves are controlled by a single manually operated switch that is connected to a timer, which is set for the desired test duration. When the specimen is in place, the test chamber is purged of air by argon admitted through a manually operated valve at the top of the chamber. This valve is closed manually, and argon is then passed through the nozzle onto the specimen. In this locally inert environment, the specimen is brought up to temperature and held there while the system stabilizes and the specimen is conditioned. Meanwhile, the reagent gases flow through the orifices into the mixing chamber but are vented from the chamber by valve 3 and are prevented from entering the nozzle by valve 2 (see Fig. 1). The gases are vented to keep the mixing chamber near atmospheric pressure, thereby minimizing pressure transients at the orifice outlets when the solenoid valves operate.
4. When the specimen reaches the desired temperature (as determined by the operator viewing it through the disappearing-filament pyrometer), the operator throws a toggle switch, which simultaneously terminates the flow of argon through the nozzle, closes the vent valve, opens solenoid valve 2 between the mixing chamber and the nozzle, and starts the clock. These conditions persist for the duration of the test (during which the operator holds the temperature of the specimen constant by controlling the Variac). At the end of the test, the heater power is automatically turned off by the timer, and the solenoid valves are switched to their pretest conditions.
5. The specimen is removed, weighed, and measured.

5. DATA REDUCTION

Recession rates ($\dot{y}$) have been measured as functions of surface temperature, impinging gas composition, and gas velocity. Eight tests were duplications of previously run tests (Table 2); the measured recession rates for those cases differ from each other by an average of 6% and at most by 15%.

The average recession rate based on measured thickness change is

$$\dot{y}_t = (y_0 - y_f)/t_f - t_0) \ , \qquad (1)$$

where y is thickness, t is time, and subscripts 0 and f designate initial and final conditions.

An "equivalent recession rate ($\dot{y}_m$) is computed from the mass loss:

$$\dot{y}_m = (m_0 - m_f)y_0/[m_0(t_f - t_0)] \ . \qquad (2)$$

The ratio $\dot{y}_m/\dot{y}_t$ is plotted in Fig. 8 as a function of total recession based on mass loss (y_m), where $y_m = \dot{y}_m(t_f - t_0)$. Figure 9 indicates that $\dot{y}_m$ is consistently greater than $\dot{y}_t$ because of the development of an 8 mil (0.2 mm) deep, 50% void, porous region at the surface (Fig. 8). Assuming that the depth of this layer remains constant as recession continues, then

$$\dot{y}_m/\dot{y}_t = y_m/(y_m - 0.008 \times 0.5) \ . \qquad (3)$$

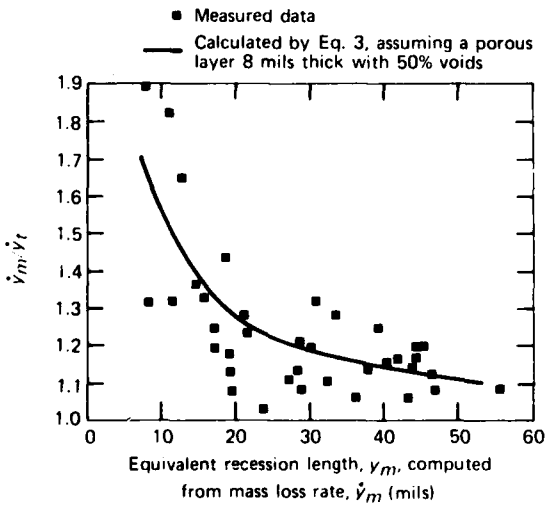

Figure 9 — Ratio of equivalent ATJ graphite recession rate measured by mass loss method to that measured by thickness change.

These calculated values are in good agreement with experimental data (Fig. 9), indicating that the porous layer remains nearly constant.

When total recession is large compared with the 8 mil porous layer, $\dot{y}_m/\dot{y}_t$ approaches unity. Most ablation tests reported in the literature use large samples and have large total recessions; $\dot{y}_m/\dot{y}_t$ approaches 1 for those cases. Since thickness measurements are difficult and the mass loss method is more representative of the amount of material ablated, the "recession rates" presented in the rest of this report are $\dot{y}_m$.

The test results plotted in Fig. 10 cover a large span of test conditions. The effect of gas velocity can be removed from these data if the recession rates are normalized by dividing $\dot{y}_m$ by h_i/ρ, where h_i is the local enthalpy-based heat transfer coefficient. The

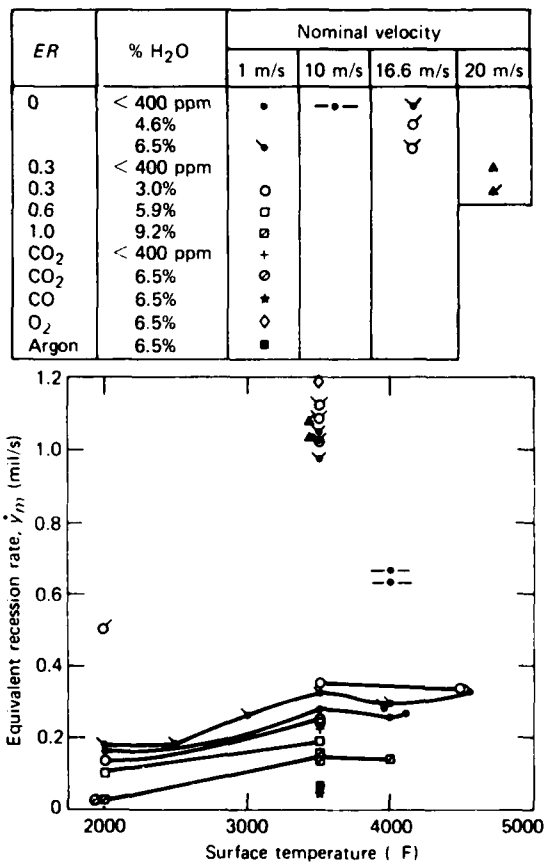

Figure 10 — Recession rate of ATJ graphite samples.

new quantity is known as the mass transfer parameter, β':[3]

$$\beta' = \frac{\dot{y}_m \rho}{h_i} = \frac{\dot{m}}{h_i} , \quad (4)$$

where

ρ = density of virgin sample, and
$\dot{m}$ = mass loss rate per unit area.

In our experiment, h_i is calculated from a formulation[4] for flow from a nozzle impinging on an infinite flat plate:

$$h_i = 0.73b(Bg\mu_\infty \rho_\infty)^{0.5}(\mu_\infty \rho_\infty / \mu_w \rho_w)^{0.5} / \mathrm{Pr}^{0.666} \quad (5)$$

where

b = blowing correction factor = $[\ln(1 + \beta')]/\beta'$,

B = velocity gradient = $1.5\ U_\infty x/d^2$ (s^{-1}) ,

g = gravitational constant (32.2 lbm-ft/lbf-s^2) ,

Pr = The Prandtl number $(c_p \mu/k)_\infty$,

μ_∞ and μ_w = freestream and wall gas viscosities (lbf-s/ft^2) ,

ρ_∞ and ρ_w = freestream and wall gas densities (lbm/ft^3) ,

U_∞ = the velocity leaving the nozzle (ft/s) ,

d = the nozzle diameter (ft) , and

x = the distance from the nozzle to the specimen (ft) .

The freestream temperature (T_∞) of the gas as it leaves the nozzle is difficult to measure, and ρ_∞, μ_∞, and U_∞ are all calculated from it. Because of heat from the boron nitride nozzle, T_∞ can be substantially above room temperature. Late in the test series, a radiation-shielded thermocouple was inserted along the nozzle axis to measure the T_∞ of the gas at the nozzle exit. Those measurements were used as a calibration to deduce the gas temperature for all of the ablation tests and for any specimen temperature and gas velocity. Figure 11 shows T_∞ versus ATJ graphite surface temperature for several "nominal" air flow velocities calculated from measured gas mass flow rates, assuming the gas

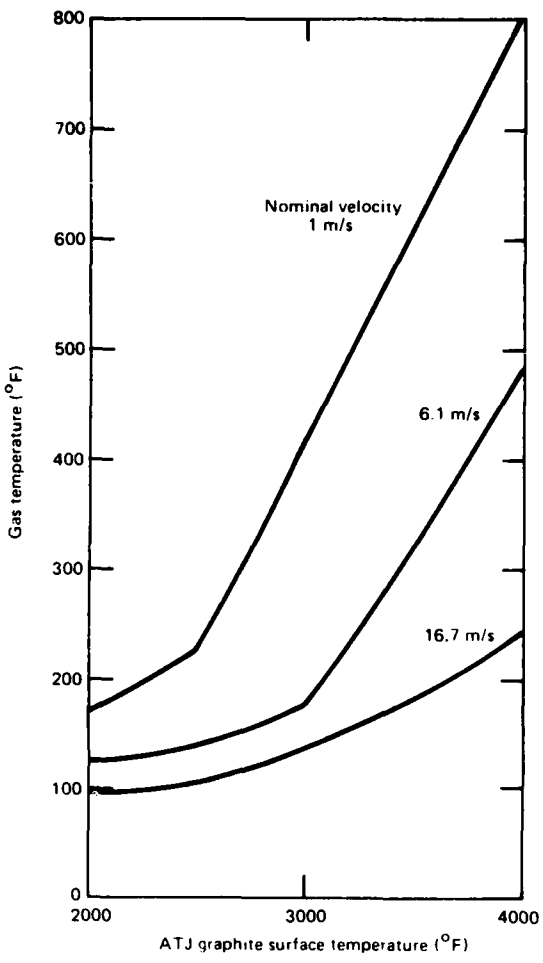

Figure 11 — Measured gas temperature at nozzle exit plane.

leaves the nozzle exit plane at room temperature. The actual velocity (U_∞) is estimated by multiplying the nominal velocity by T_∞ / T_{room}. One should remember, however, that T_∞ is difficult to measure accurately because the sample and heater surfaces radiate heat to the thermocouple, thereby introducing error. Although the thermocouple is shielded, the shielding method allows some reflected radiation to reach the thermocouple. Consequently, measured temperatures are higher than the actual gas tem-

[3] L. L. Perini, *Review of Graphite Ablation Theory and Experimental Data*, JHU/APL ANSP-M-1 (Dec 1971).

[4] I. A. Belov, "The effect of Turbulence on Heat-Exchange in a Jet Meeting an Obstacle," translated from *Teplo i Massoperenos* (1969), British Library Lending Division.

perature, especially when surface temperature is high and gas flow rate is low. Fortunately, h_i is not a strong function of T_∞, since it is proportional to $\mu_\infty \rho_\infty \sqrt{U_\infty}$, where μ_∞ and U_∞ increase with temperature and ρ_∞ decreases with temperature. When the nominal velocity is 1 m/s and the surface temperature is 3500°F, the effect of reducing T_∞ from 610 to 70°F is to reduce h_i by 15%.

The blowing correction factor (b) accounts for the ablating combustion gases increasing the boundary layer thickness and reducing the heat transfer coefficient. In the present tests, β' is usually less than 0.2; therefore, the blowing correction is usually less than 10%.

6. TEST RESULTS

Simulated Shelldyne-Air

Shelldyne-air combustion gas products are simulated using measured amounts of O_2, N_2, CO_2, CO, and water vapor. The gas compositions shown in Table 3 are computed by the NOTS computer program,[5] assuming chemical equilibrium and that combustion occurs at 1 atm and with an initial air total temperature of 620°F. At the higher *ER*'s, there are relatively high concentrations of CO_2 and water vapor and low concentrations of free O_2. Figure 12 shows that β' increases with decreasing *ER* because low *ER*'s have more O_2 available to react with the ablating surface. At the diffusion limit, the effect of O_2 availability on ablation rate can be calculated as follows, assuming that O_2 and CO_2 in the stream react with carbon at the surface to form CO:[3]

$$\beta'_d = \dot{m}_d/h_i = (\dot{m}_1/\dot{m}_{O_2})\alpha_{O_2} + (\dot{m}_2/\dot{m}_{CO_2})\alpha_{CO_2} , \quad (6)$$

where

β'_d = diffusion limited mass transfer parameter (kinetic reaction rates assumed to be infinite);

$\dot{m}_d$ = diffusion limited mass loss rate;

$\dot{m}_1$, $\dot{m}_2$ = theoretical mass loss rates of carbon from the ablating surface owing to reactions with O_2 and CO_2, respectively;

$\dot{m}_{O_2}$, $\dot{m}_{CO_2}$ = mass flow rates of O_2 and CO_2 reacting with carbon;

α_{O_2}, α_{CO_2} = mass fractions of O_2 and CO_2 in the incoming gas stream (weight%) (for dry air, $\alpha_{O_2} = 0.23$, $\alpha_{CO_2} = 0$);

m_1/m_{O_2} = 12/16 = 0.75 (since $C + \frac{1}{2}O_2 \rightarrow CO$); and

m_2/m_{CO_2} = 12/44 = 0.273 (since $C + CO_2 \rightarrow 2CO$).

The mass fractions (α) are known from the gas flow composition, and the values of β'_d are calculated as shown in Table 4. From Fig. 12, β' for *ER* > 0 is slightly greater than β'_d at 3500°F and substantially less than β'_d at 2000°F. Normalizing β' by β'_d (Fig. 13a) greatly reduces the spread in the data, with most of the 3500°F ratios around 1.1 (in reality β'/β'_d must be ≤ 1.0), and the 2000°F ratios are around 0.75. Ratios less than 1.0 indicate that not all the O_2 and CO_2 available at the surface is reacting with ATJ graphite to produce CO. If we assume that none of the CO_2 in the gas stream reacts with the surface (i.e., if $\dot{m}_2 = 0$ in Eq. 6), the β'/β'_d ratios at 3500°F exceed unity for all *ER*'s > 0 (Fig. 13b).

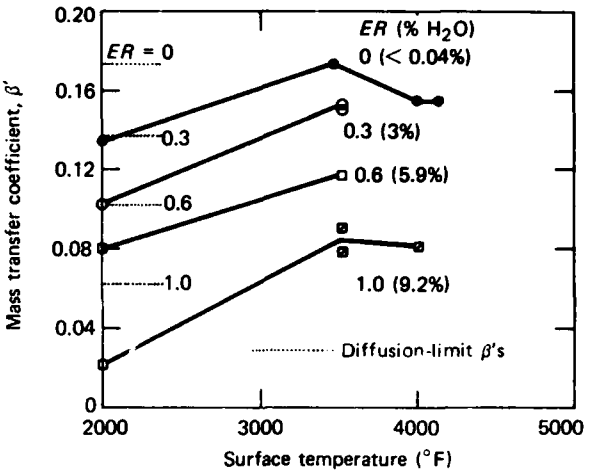

Figure 12 — Measured mass transfer coefficients for ATJ graphite samples exposed to simulated Shelldyne-air gas flowing at a nominal velocity of 1 m/s.

Since β'/β'_d should always be less than 1.0, the ratio of approximately 1.4 at *ER* = 1.0 in Fig. 13a must be due either to experimental error or to carbon reacting at the surface with gases other than O_2 and CO_2; i.e., H_2O, N_2, or nitrous oxide (NO). If we arbitrarily assume all available water vapor in the gas reacts with the surface to form CO, a new β'_d can be calculated for each *ER* (Table 4). The resulting β'/β'_d rates are substantially less than 1.0 at the higher *ER*'s (Fig. 13c). Therefore, let us modify our assumption and postulate that half the water vapor reacts to form CO (or that all the water vapor reacts to form CO_2). With this assumption, the β'/β'_d ratios at 3500°F are very close to 1.0 (Fig. 13d).

[5] D. R. Cruise, "Notes on the Rapid Computation of Chemical Equilibria," *J. Phys. Chem.* **68** (12), 3797-3802 (Dec 1964).

Table 3 – Calculated gas compositions and flame temperatures of reacted Shelldyne-air; incoming air total temperature, 620°F; combustion occurs at 1 atm pressure.

Simulated ER	*Gas Composition*							*Flame Temp. (°F)*
		NO	O_2	N_2	CO_2	*CO*	H_2O	
0.3	mole %	–	14.5	77.8	4.7	–	3.0	1978
	wt %	–	16.0	75.0	7.1	–	1.9	
0.6	mole %	0.2	8.0	76.6	9.3	–	5.9	3079
	wt %	0.2	8.8	73.4	13.9	–	3.7	
1.0	mole %	0.3	0.8	74.2	13.2	1.8	9.2	3606
	wt %	0.3	0.9	71.3	19.9	1.7	5.7	

Table 4 – Calculated diffusion-limited mass transfer coefficients (β'_d).

*Per Eq.**	*Simulated Shelldyne ER*				*Gases with 6.5% H_2O by Volume*					*100% CO_2*
	Dry Air	0.3	0.6	1.0	CO_2	*CO*	O_2	*Argon*	*Air*	
1,2	0.1725	0.139	0.104	0.061	0.265	0	0.722	0	0.1651	0.273
1	0.1725	0.12	0.066	0.068	0	0	0.722	0	0.1651	0
1,2,3	0.1725	0.152	0.129	0.099	0.286	0.032	0.746	0.050	0.194	0.273
1,2,4	0.1725	0.145	0.116	0.080	0.275	0.016	0.734	0.025	0.179	0.273

*$O_2 + 2C \rightarrow 2CO$ (1)
$CO_2 + C \rightarrow 2CO$ (2)
$H_2O + C \rightarrow H_2 + CO$ (3)
$2H_2O + C \rightarrow 2H_2 + CO_2$ (4)

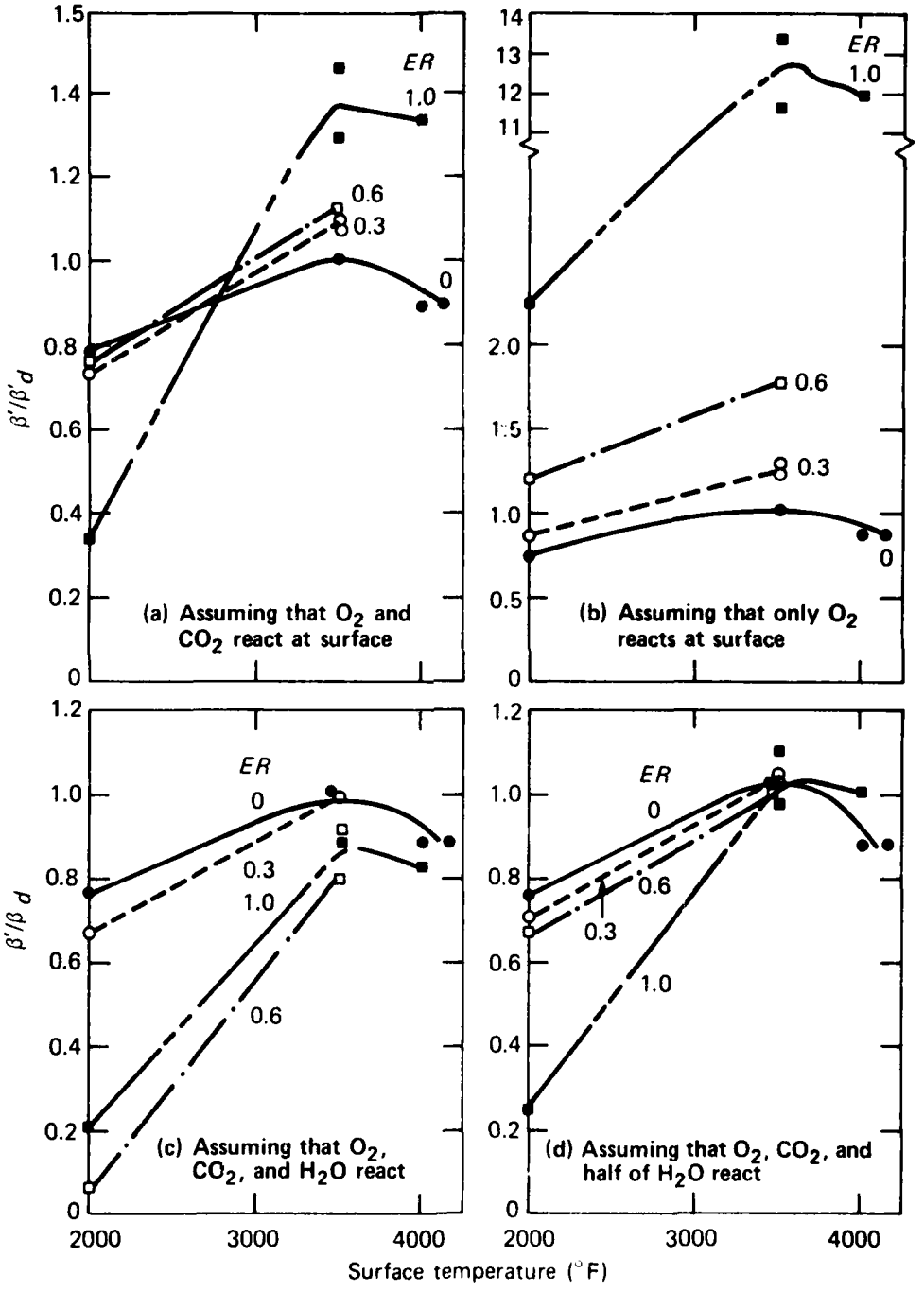

Figure 13 — Ratio of measured mass transfer coefficient to diffusion-limited mass transfer coefficient for ATJ graphite samples exposed to Shelldyne-air flows.

Although the chemical mechanisms are as yet unknown, it appears that at 3500°F water vapor is reacting with the surface in a manner similar to our second postulation. This is also shown in Fig. 14 where recession rates at 3500°F and a nominal velocity of 1 m/s are plotted versus *ER*.

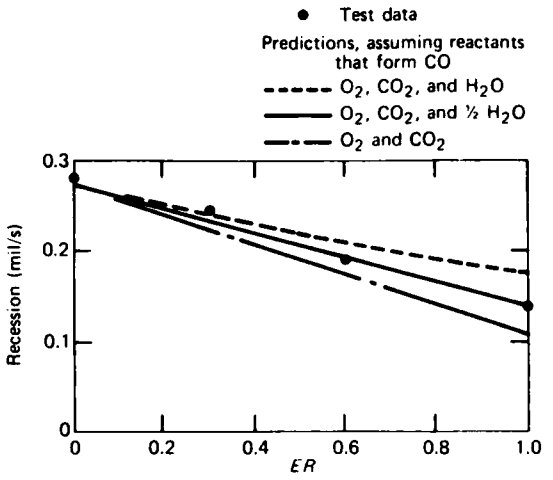

Figure 14 — Recession of carbon in Shelldyne-air mixtures; surface temperature, 3500°F; flow normal to surface at 1 m/s.

Thus, our data indicate that CO_2 and H_2O have significant reactions with the surface. This is important since previous analyses[6] have assumed that CO_2 and H_2O in the gas stream do not react with the surface. It is particularly important when combustor gases are near $ER = 1.0$, since in those cases ablation rates are primarily determined by the CO_2 and H_2O reactions at the surface. However, one should realize that the velocity of the burned gas in the combustor will be on the order of 1000 m/s, and parallel to, rather than normal to, the wall, which may affect the degrees of reaction of CO_2 and H_2O. Future analysis and experimentation will attempt to determine the extent of these effects.

Velocities Greater than 1 m/s

A limited amount of data (mostly with air) has been taken at nominal velocities greater than 1 m/s. Figure 15 (from Ref. 3) shows that for air, β'/β'_d should be independent of T_{wall} in the 3000 to 5000°F range. With this in mind, Fig. 16 shows that β'/β'_d also appears to be independent of U_∞ in this temperature range. The data at $U_\infty = 2$ and 20 m/s are very close to β'/β'_d of 1.0. The fact that the limited data at 10 m/s are at 0.8 may simply indicate experimental error.

Effects of Water Vapor and Specimen Temperature on Tests with Air

For the 19 tests with air at nominal velocities between 1 and 16.6 m/s, the β'/β'_d ratios are in good agreement with the results of Golovina and Khaustovich[7] who tested carbon electrode spheres in heated air (Fig. 17). This figure shows that the carbon-air reaction reaches a diffusion limit around 3000°F and at lower temperatures is rate controlled, with significant ablation occurring as low as 1500°F. The good agreement with the Ref. 7 data gives us added confidence in our test apparatus and procedures.

Carbon Dioxide Gas Flow

Prior to the current series of tests, our thermochemical computer model assumed that at low to moderate temperatures, the reaction rate for CO_2 with graphite is low enough that the CO_2 will be swept away from the surface before it has a chance to react. However, tests with CO_2 and H_2O flows indicate that CO_2 reacts at temperatures as low as 2000°F.

Table 1 shows that the ablation rates for CO_2 at 3500 and 4500°F are similar to those for air, either dry or with 6.5% water. Reducing the water vapor content in the CO_2 gas to less than 0.04% reduces the ablation rate by 35%.

At 2000°F, the mixture of 93.5% CO_2 and 6.5% H_2O has a low ablation rate (Fig. 18). This agrees with the data for electrode carbon, presented in Ref. 7, which reported a β'/β'_d of 0.02 at 2000°F.

No mention is made in Ref. 7 of the water concentration in the CO_2. At 3500°F, the CO_2 – 6.5% H_2O data are within the range of data from Ref. 7, while the data for CO_2 with less than 0.04% H_2O are 25% lower than the values in Ref. 7. Additional information is needed about the water content of

[6] R. W. Newman and H. G. Fox, "Supersonic Combustor Insulation Ablation Analysis and Tests," presented at 12th Navy Symposium on Aeroballistics, David Taylor Naval Ship R&D Center, Carderock, Md. (12-14 May 1981).

[7] E. S. Golovina and G. P. Khaustovich, "The Interaction of Carbon with Carbon Dioxide and Oxygen at Temperatures up to 3000°K," in *Eighth Symposium on Combustion*, Williams and Wilkins (1962).

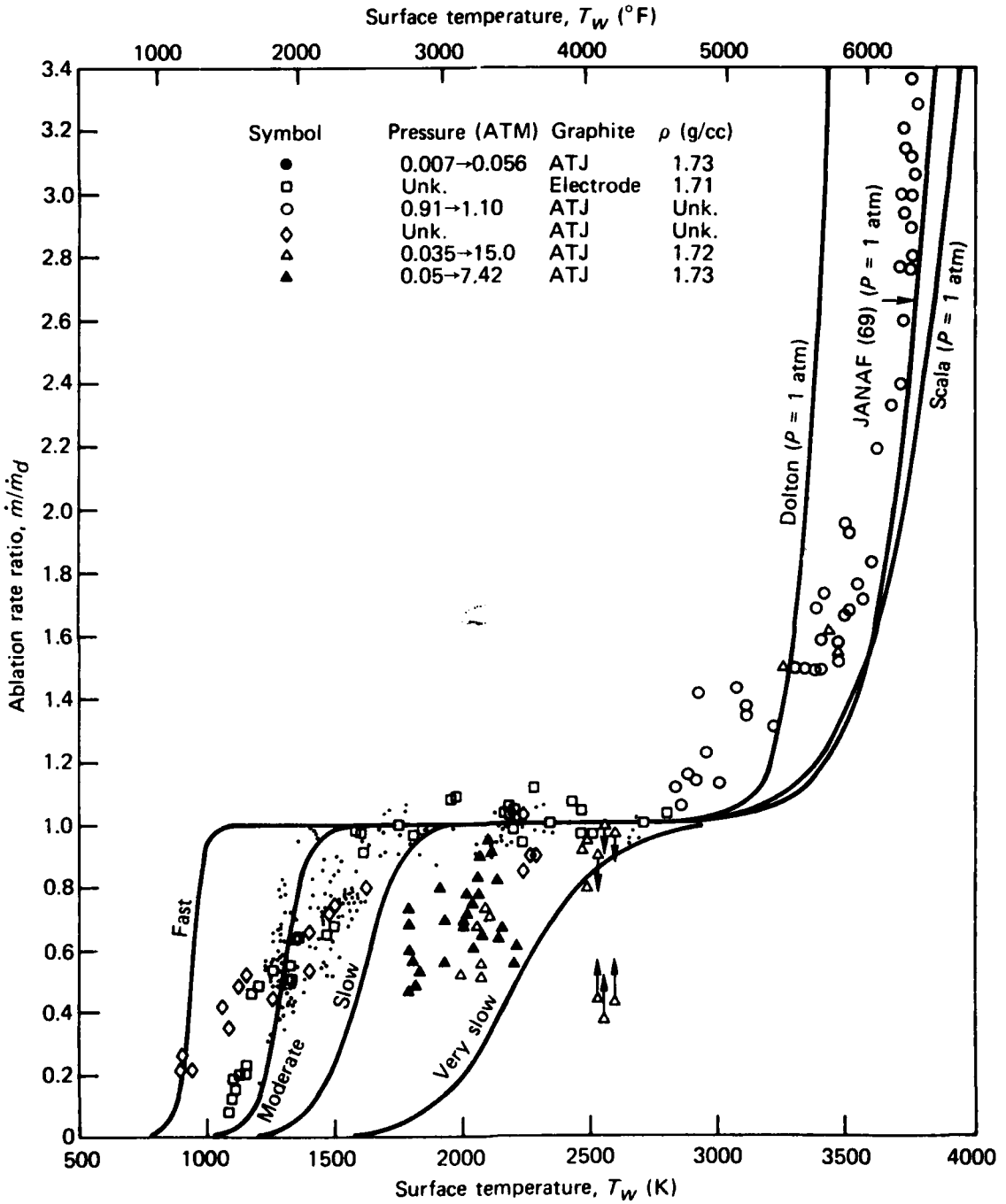

Figure 15 — Review of available graphite ablation test data (Ref. 3).

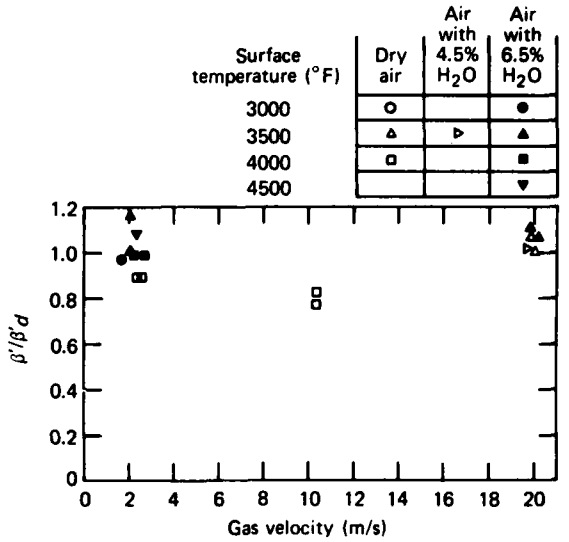

Figure 16 — Ratio of mass transfer coefficient to diffusion-limited mass transfer coefficient for ATJ graphite samples exposed to air, assuming that O_2 and half of H_2O react to form CO.

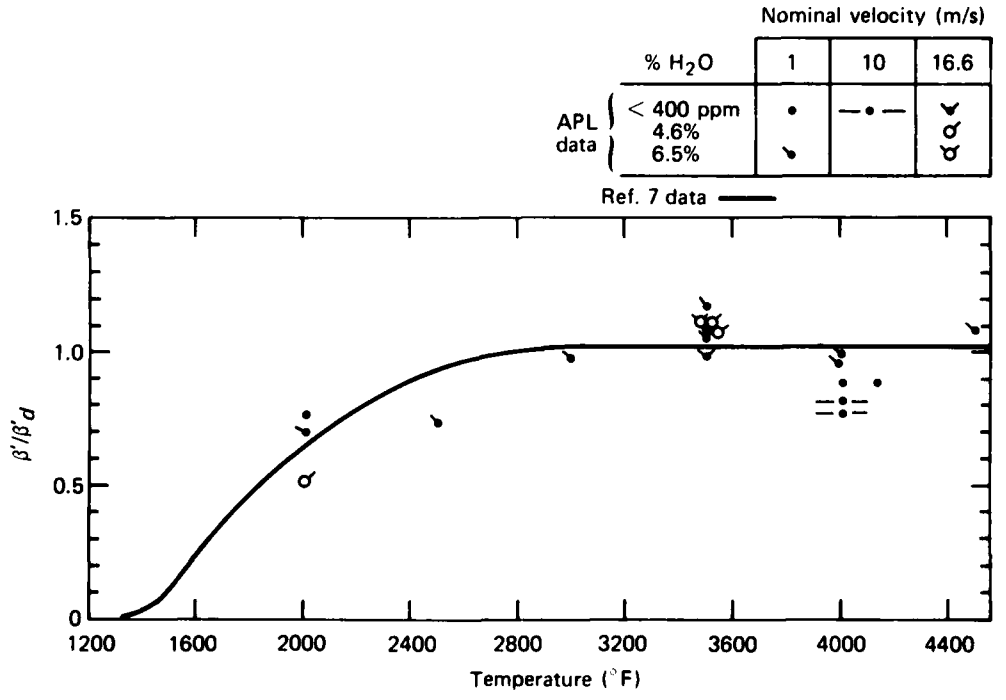

Figure 17 — Comparison of present air flow ablation data with Ref. 7 data.

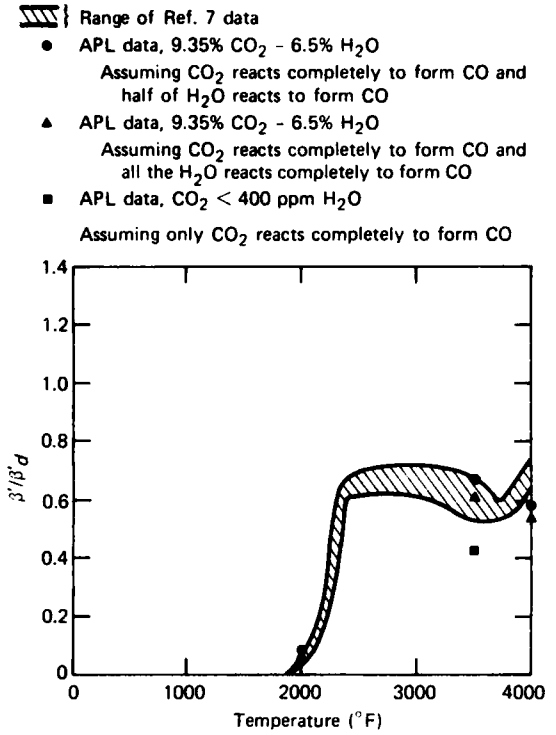

Figure 18 — Ratio of mass transfer coefficient to diffusion-limited mass transfer coefficient for ATJ graphite samples exposed to CO_2 and H_2O gas mixtures flowing at a nominal velocity of 1 m/s.

CO_2 in Ref. 7, and more data from our test apparatus are required for a better comparison. The data show that CO_2 reacts with the carbon surface, even at temperatures as low as 2000°F. However, since β'/β'_d is less than 1, not all the available CO_2 is reacting.

Carbon Monoxide and Argon Gas Flow

Two tests were run at 3500°F using inert CO and argon gas flows, each containing 6.5% by volume of water. The test data show recession rates of 0.052 mil/s for CO – 6.5% H_2O and 0.059 mil/s for argon – 6.5% H_2O (Fig. 10). Previous tests in our apparatus with 100% argon gave no measurable mass loss. Apparently at 3500°F, water vapor reacts with carbon, as was noted earlier. Assuming that each oxygen atom in water reacts to form CO, then the β'/β'_d ratio is very nearly 1.0 for the CO – water vapor mixture. However assuming CO_2 is formed (or, equivalently, that only half the oxygen in water reacts to form CO), then β'/β'_d is more than 2.0. Since β'/β'_d ratios greater than 1.0 cannot occur, all the water vapor must be reacting to form CO. For the argon – 6.5% H_2O gas, it appears that only half of the available water is reacting to form CO (or, equivalently, it is all reacting to form CO_2), because the β'/β'_d ratio is near 1.0. This value agrees with our tentative findings for Shelldyne-air gas flows.

Oxygen Gas Flow

Only one test was run for an O_2 – 6.5% H_2O gas. The recession rate was very high (1.2 mils/s at 3500°F). Assuming that O_2 reacts with the surface to form CO results in a β'/β'_d ratio of 1.23. If the H_2O is also assumed to react to form CO, the ratio is reduced slightly to 1.19. The ratio is greater than 1.0; therefore, either our assumptions for computing β' and/or β'_d are incorrect or the difference is caused by experimental error.

Comparison with Matsui Data

Matsui et al.[8] heated the backfaces of ATJ graphite samples with an acetylene burner to temperatures up to 2800°F. Although their data were taken at slightly different velocity gradients than ours, Fig. 19 shows relatively good agreement between the two sets of data.

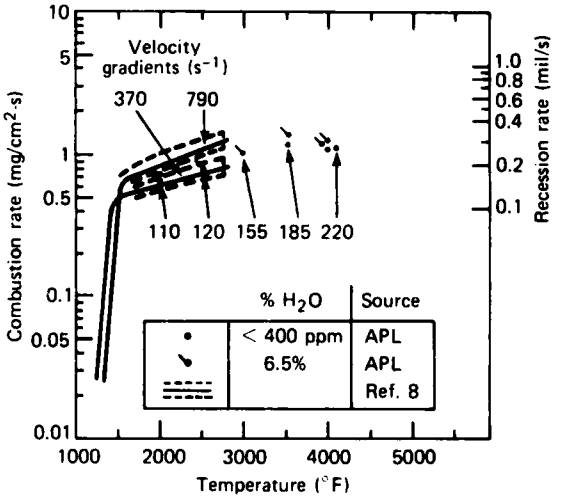

Figure 19 — ATJ graphite combustion rate in air versus temperature.

[8] K. Matsui et al., "Fluid-Mechanical Effects on the Combustion Rate of Solid Carbon, *Combust. Flame* **25**, 57-66 (1975).

7. CONCLUSIONS

A test apparatus and procedure have been developed to measure ablation rates on high-temperature graphite samples exposed to the normal flow of various gases. Using this apparatus, tests have been performed on ATJ graphite samples at temperatures up to 4500°F exposed to various gas mixtures. The following conclusions can be drawn about these tests:

1. Ablation rates measured for air agree well with data presented in the literature (Figs. 17 and 19). This good correlation provides confidence in the test procedure.
2. Tests were performed in which the graphite was exposed to simulated Shelldyne-air combustion products for *ER*'s of 0.3, 0.6, and 1.0. The results indicate that, at 3500°F, the CO_2 in the gas mixture reacts with the surface at close to the diffusion-limited rate (Fig. 13d). At 2000°F, the CO_2 reacts at about one-half this rate. The data also indicate that about half of the water in the gas mixture reacts with the surface at 3500°F, but inadequate data were taken at 2000°F to draw any conclusions.
3. Recession rate data taken at various gas velocities correlate well with the theory that in the diffusion limit, the ablation rate is directly proportional to the enthalpy-based heat transfer coefficient, h_i (i.e., $\dot{m}_d = h_i \beta'_d$, where h_i is a function of gas velocity).
4. Some tests were conducted in which the graphite was exposed to CO, CO_2, argon, and O_2, all with 6.5 mole% H_2O. Results of these tests (see Table 1) show that both CO_2 and H_2O react with the graphite heated to only 2000°F. This is especially important for high *ER* gas flows for which little O_2 is available but where there is an abundance of CO_2 and H_2O. Previous thermal analyses of materials under these conditions will be reanalyzed using a reacting CO_2 and H_2O chemical model.

8. PLANNED WORK

Although the data obtained so far appear to be in good agreement with data in the available literature, the quantity is limited to only one or two data points per test condition in most cases. Plans are being made to obtain the additional data needed to support the conclusions made in this study. In addition, tests will use coherent anti-Stokes Raman spectroscopy to measure species concentrations at the ablating surface and in the boundary layer. This information will add to our knowledge of the chemical reactions occurring near the ablating surface. Also, support is being solicited from NAVSEA to perform ablation measurements on carbon-carbon composites.

ACKNOWLEDGMENTS

The work reported herein is sponsored by APL IR&D funds. The authors appreciate the guidance given by L. B. Weckesser, L. L. Perini, and R. M. Fristrom and wish to thank B. J. Prosen for her assistance. They also wish to thank L. B. Weckesser and G. L. Dugger for their considerable editorial efforts in the review of this report.

REFERENCES

[1] C. H. Hoshall, *Graphite Ablation Tests,* JHU/APL CFP-80-003 (15 Jan 1980).

[2] R. W. Newman, *Test Plan to Measure High Temperature Graphite Ablation Rate,* JHU/APL EM-4999 (26 Jun 1981).

[3] L. L. Perini, *Review of Graphite Ablation Theory and Experimental Data,* JHU/APL ANSP-M-1 (Dec 1971).

[4] I. A. Belov, "The effect of Turbulence on Heat-Exchange in a Jet Meeting an Obstacle," translated from *Teplo i Massoperenos* (1969), British Library Lending Division.

[5] D. R. Cruise, "Notes on the Rapid Computation of Chemical Equilibria," *J. Phys. Chem.* **68**(12), 3797-3802 (Dec 1964).

[6] R. W. Newman and H. G. Fox, "Supersonic Combustor Insulation Ablation Analysis and Tests," presented at 12th Navy Symposium on Aeroballistics, David Taylor Naval Ship R&D Center, Carderock, Md. (12-14 May 1981).

[7] E. S. Golovina and G. P. Khaustovich, "The Interaction of Carbon with Carbon Dioxide and Oxygen at Temperatures up to 3000°K," in *Eighth Symposium on Combustion,* Williams and Wilkins (1962).

[8] K. Matsui et al., "Fluid-Mechanical Effects on the Combustion Rate of Solid Carbon, *Combust. Flame* **25**, 57-66 (1975).

THE JOHNS HOPKINS UNIVERSITY
APPLIED PHYSICS LABORATORY
LAUREL, MARYLAND

APPENDIX A

DATA RECORDING SYSTEM

Presented below are discussions of the instrumentation and recording equipment used in this test program.

Channel 1 and Channel 2, Gas Pressure

Two identical 0 to 200 psi transducers are used (Fig. 1). Excitation voltages (+15, −15 VDC) are provided by a modular power supply. The transducers were first calibrated (output voltage versus percent full-scale pressure) at the APL Propulsion Research Laboratory. The data were then plotted to assist in an evaluation of the linearity of the output voltage versus pressure in the range of pressures (20 to 80 psig) anticipated in the current test series. The linearity appeared to be sufficient that output voltage could be calculated for pressures at intervals of 5 psig. The transducers were connected to a compressed air supply in which the pressure could be set as required to provide output voltages (read with a digital multimeter) corresonding to pressure at 5 psig intervals. The electrical outputs of the transducers for each pressure were recorded on the Visicorder. Deflections of the Visicorder trace were scaled, and calibration scales indicating psig as a function of Visicorder deflection were made so that pressures could be read directly from the Visicorder records. When tests were run, pressures were read from the Visicorder chart and the values were used to calculate gas flow by means of tables of orifice constants.

Channel 3, Heater Current

The magnitudes of heater current and voltage were recorded so that the amount of power consumed by the heater could be determined. During the course of runs in which the heater (as well as the specimen) was ablated, the heater power needed to maintain temperature varied considerably. The heater is assumed to be purely resistive, and current and voltage are assumed to be in phase.

A 0.33 mΩ (50 mV at 150 A) shunt was connected in the cable through which power is supplied by the 5 kVA transformer to the heater (Fig. 1). Amplification in addition to that provided by the plug-in module of the Visicorder was required in order to provide trace deflections of reasonable amplitude; the amplifier section of a Vishay Model 2120 Strain Gage Conditioner module was used to amplify the AC signal appearing across the shunt by a factor of 100 before it was rectified and filtered. This method provided a simple way to record a thin-line trace (rather than an AC waveform), thereby causing minimal interference with other traces.

This channel was calibrated by manually setting the Variac (Fig. 2) to provide heater currents at increments of approximately 10 A throughout the range (0 to 130 A) anticipated as a requirement to raise the heater to 5000°F. With the Vishay amplifier set for a gain of 100, the voltage across the shunt was read on a Data Precision Model 258 digital multimeter (which has a 0 to 100 mV AC range) and was recorded simultaneously on the Visicorder. From these data, a plot of Visicorder deflection (ordinate) versus shunt voltage (abscissa) was made. Since shunt voltage and heater current are directly and linearly related, the abscissa can be calibrated as heater current, thus providing a curve showing the relationship of the Visicorder deflection to current. It was not possible in all cases to set the Variac for predetermined values of current. It was also difficult to obtain steady readings – hence this somewhat indirect calibration technique.

Channel 4, Heater Voltage

Heater electrode voltage was recorded by attaching fiberglass-insulated buss wire leads directly to the clamps in which the heater electrode is held. A half-wave rectifier/filter/voltage divider (as in the heater current channel) provides a thin-line trace. For this calibration, the heater electrode was removed and the Variac was set to provide various voltages on the heater clamps. The voltage was read with a Data Precision Model 258 digital multimeter and was recorded simultaneously by the Visicorder. A calibration scale of trace deflection versus voltage was then made so that electrode voltage could be read directly from the Visicorder charts.

Channel 5, Reagent On

A mark along the edge of the Visicorder chart indicates when the TEST GAS switch is turned on and the reagent gas is presumed to be flowing through the nozzle and onto the heated specimen. When the argon is switched off by the solenoid valves and the reagent gas begins to flow through the nozzle, the REAGENT ON trace begins to darken a strip approximately 0.125 in. (3.2 mm) wide along one edge of the Visicorder record. This continues until the timer (Fig. 2) reaches zero and turns the heater power off and operates the solenoid valves, turning the reagent gas off and the argon on, thus terminating the test run.

The REAGENT ON indication is provided by an AC voltage from the valve control circuit and is not calibrated. The position control of the Visicorder amplifier is adjusted so that the trace is positioned completely off the chart when the reagent is off and the peaks of the AC waveform darken the edge of the chart when the reagent is on.

Channel 6, Nozzle Gas Temperature

This channel is dedicated to recording the output voltage of a thermocouple in the reagent gas stream at the nozzle exit. It was not used in these tests because the thermocouple was not incorporated into the apparatus until late in the series. The thermocouple measurements were used to prepare a calibration (Fig. 11) relating gas temperature to the graphite specimen temperature and the gas flow velocity. By means of an iteration process, the gas velocity was determined by multiplying the room temperature velocity by the ratio of the gas static temperature to room temperature.

Channel 7, Photovoltaic Pyrometer

For these tests, the photovoltaic (PV.) pyrometer was aimed at the center of the surface of the pellet through the viewing window at the top of the test chamber. The image of a small aiming circle that is visible to the operator is very useful in this process.

The PV. pyrometer provides a continuous record of specimen temperature. For these tests, it was calibrated by using the disappearing filament (D.F.) pyrometer as the standard. (For details of the calibration, refer to Appendix B.) Amplification of the output of the PV. pyrometer in addition to that provided by the Honeywell 1833A-MPD modules (50 mV/division) was required. Amplifications of from 100 to 1100 were provided by the amplifier section of the Vishay Model 2120 Strain Gage Conditioner module.

To calibrate the PV. pyrometer, both pyrometers were aimed through the viewing window at the same area (approximately 0.1 by 0.1 in., or 2.5 by 2.5 mm) on the tip of a heater electrode that was not counterbored (Fig. 20b). The D.F. pyrometer current was preset for each temperature at which a calibration measurement was to be made. The test chamber was then purged with argon, the Visicorder was started, and power was applied to the heater electrode. Heater power was increased steadily until the tip of the filament of the D.F. pyrometer "disappeared," providing an indication that the heater was at the desired temperature. The heater was observed through the D.F. pyrometer for a few seconds as a short length of Visicorder record was made. Power to the heater was then turned off. This process was repeated at 250°F intervals in the range of 2000 to 5000°F.

The deflection from the cool-electrode baseline for each temperature was then scaled, and a plot was made of temperature (ordinate) versus deflection (abscissa). Test data were later reduced by measuring the deflection with an engineer's scale and reading the temperature from the curve.

The PV. pyrometer output is very nonlinear (as a function of temperature). It was necessary to prepare calibration curves for five combinations of amplifier gain and Visicorder sensitivity so as to use deflections of reasonable amplitude throughout the temperature range of interest.

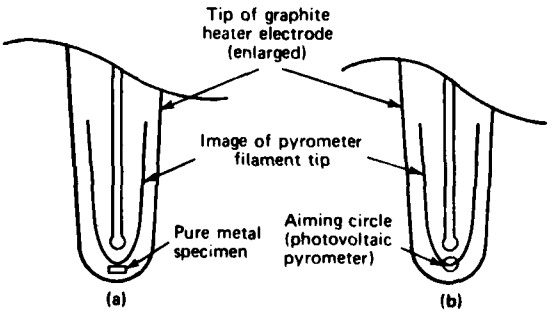

Figure 20 — Aiming procedure for pyrometer calibration. (a) Pure metal melting point calibration of D. F.-pyrometer. (b) PV. versus D. F. calibration.

Channel 8, Disappearing-Filament Pyrometer

This channel recorded the filament current (amplitude) of the D.F. pyrometer. A precision resistor was connected in series with the instrument filament (Fig. 1), and the voltage across the resistor was recorded. To calibrate the recorder, the filament current (as read on a Model 245 Data Precision digital multimeter) was set at 48 mA (the lowest calibration point on the meter originally provided with the instrument), at 50 mA, then at increments of 5 mA up to 85 mA, and finally at 86 mA (the upper calibration point on the meter). A scale for determining current amplitude from future records was made from the Visicorder chart. The deflection was linear (as a function of current) so that the scale could be subdivided equally (between the 5 mA increments) to provide 1.0 and 0.5 mA gradations.

APPENDIX B

PYROMETER CALIBRATION

One of the basic calibrations and one upon which other critical calibrations are based is that of the disappearing-filament (D.F.) pyrometer. A Pyro Micro-Optical Pyrometer made by Pyrometer Instruments Co., Inc., Bergenfield, N.J., was used. This instrument can be seen in the foreground in Fig. 2.

The term "disappearing filament" is derived from the fact that the temperature of the specimen is measured by matching the color and brightness of the hot specimen with a standard by superimposing an image of a heated filament inside the instrument upon an enlarged image of the specimen. Current supplied by a power supply external to the instrument (Fig. 1) is passed through the filament, heating it and causing it to glow. The operator views the specimen and the image of the filament through the eyepiece and adjusts the filament current until the color and intensity of the tip of the filament match that of the specimen and so "disappear," i.e., blend with the specimen so that it is not visible. In this way, the temperature of the specimen can be determined rather accurately by measuring the current flowing through the filament at the time of the color match.

A calibration curve of specimen temperature versus filament current was established by recording filament currents that correspond to accurately known melting points of pure metals. The calibration was accomplished by placing small lengths of various pure metal wires, 0.001 to 0.010 in. (0.025 to 0.25 mm) in diameter and approximately 0.04 in. (1.0 mm) long, in a small cavity in the tip of a heater electrode. The pyrometer was aimed so as to view the graphite and to position the tip of the filament as close to the metal as possible (Fig. 20a). The metal was observed carefully through the pyrometer (which provides considerable magnification) as the temperature of the heater was raised very slowly. As the temperature was being increased, the filament current was continually adjusted with the control on the pyrometer so that the tip of the pyrometer filament was not visible against the image of the graphite heater. The emissivities of all the metals were considerably lower than that of the graphite. As a consequence, all the metals appeared darker than the graphite even though – it seems reasonable to assume – the temperature of the metal was very nearly that of the heater. The pyrometer is normally calibrated to read temperatures of black bodies.

Tests in this series were to be run at temperatures ranging from 2000 to 4500°F. Pure metals on hand in the APL Combustion Research Laboratory provided reasonable calibration points. A digital multimeter was used so that errors inherent in reading analog meters (such as the one supplied with the pyrometer) would be eliminated. A record was made of the pyrometer filament current flowing at the instant the metal melted, and the process was repeated several times for each metal. The graphite heater on which the metal was resting was considered to be at the same temperature as the melting temperature of the metal. Detection of the melting point of the metal was enhanced by using a small length of wire so that the surface tension of the molten metal would cause the metal to tend to assume a spherical shape when it became molten.

These calibration techniques were used in an effort to provide reasonable accuracy in the measurement of temperatures with instruments that were available. The basic concept of basing the calibration upon the melting points of pure metals is considered to be sound and is probably as good as any method available, within the restraints for these tests. Another objective of this effort was to minimize several potential sources of error that could be encountered in an apparatus such as the one described here. The following comments and observations are made:

1. All components of the optical pyrometer system used to take data are the same as those used for calibration, including instruments, geometry (e.g., relative positions of parts of the system), distances between the pyrometer and the hot body being observed, and the optical path (which includes the viewing window and pyrometer lenses).
2. Uncertainties resulting from differences in the emissivity characteristics of different materials were minimized by making surface temperature measurements of graphite only. If the surface

temperatures of metals were observed in calibrating the pyrometer, a correction would have to be made to account for differences in the emissivity of the metals.

3. Calibration is done in an argon atmosphere but the chamber is full of the reagent and products of reaction when the tests are being run; variations in (optical) transmission characteristics inside the chamber are considered to be only a second-order effect.
4. Deposits of what appeared to be boron nitride from the nozzle and/or heater spacers were very much in evidence in some of the tests in which water vapor was present. Tests should be run to determine whether measurements are altered by deposits on the viewing window.

INITIAL DISTRIBUTION EXTERNAL TO THE APPLIED PHYSICS LABORATORY*

The work reported in TG 1336 was done under Navy Contract N00024-83-C-5301. This work is related to Task X8G1, which is supported by IR&D.

ORGANIZATION	LOCATION	ATTENTION	NO. OF COPIES
DEPARTMENT OF DEFENSE			
Defense Technical Information Center	Alexandria, VA	Accessions	12
DEPARTMENT OF THE NAVY			
NAVSEASYSCOM	Washington, DC	SEA-062R	1
Office of Naval Research	Washington, DC	L. H. Peebles, Jr., Code 431	1
Naval Surface Weapons Center	White Oak, MD	M. Messick C. Roe	1
	Dahlgren, VA	F. Moore	1
Naval Weapons Center	China Lake, CA	F. Strobel, Code 3242	1
NAVPLANTREPO	Laurel, MD		
CONTRACTORS			
McDonnell Douglas Aerospace Corp.	St. Louis, MO	D. Boekemeier	1
United Technologies Corp., Chemical Systems Div.	Sunnyvale, CA	P. Melia	1
Vought Corp.	Dallas, TX	J. Medford	1

Requests for copies of this report from DoD activities and contractors should be directed to DTIC, Cameron Station, Alexandria, Virginia 22314 using DTIC Form 1 and, if necessary, DTIC Form 55.

*Initial distribution of this document within the Applied Physics Laboratory has been made in accordance with a list on file in the APL Technical Publications Group.

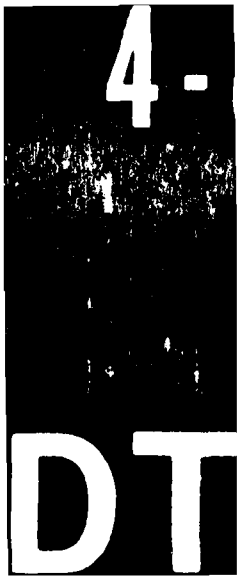
4-
DT